Spectroscopic Characterization of Charged Defects in Polycrystalline Pentacene by Time- and Wavelength-Resolved Electric Force Microscopy

ARTICLE *in* ADVANCED MATERIALS · FEBRUARY 2011

Impact Factor: 17.49 · DOI: 10.1002/adma.201003073 · Source: PubMed

5 AUTHORS, INCLUDING:

Richard G. Hennig
University of Florida
165 PUBLICATIONS **2,163** CITATIONS
SEE PROFILE

John A Marohn
Cornell University
91 PUBLICATIONS **1,108** CITATIONS
SEE PROFILE

Spectroscopic Characterization of Charged Defects in Polycrystalline Pentacene by Time- and Wavelength-Resolved Electric Force Microscopy

*Justin L. Luria, Kathleen A. Schwarz, Michael J. Jaquith, Richard G. Hennig, and John A. Marohn**

Organic semiconductors are attractive materials for microelectronic and photovoltaic applications because their energy levels, optical properties, and solubility can be independently adjusted. While significant progress towards the commercialization of organic semiconductor devices has been made, the long-term reliability of most organic semiconductors remains a concern. Charge trapping, for example, causes a wide array of functional problems in organic semiconductor devices including a reduction in mobility, an increase in off-current, and an increase in operating voltage. Yet trap formation in these materials remains poorly understood, even in pentacene, the most widely studied organic semiconductor. Proposed trapping mechanisms in pentacene include the immobilization of charge at grain boundary defects[1,2] and dielectric interfaces,[2–4] formation of immobile bipolarons,[5] and chemical reactions.[6–9] Many transistor studies indicate a degradation of device performance following exposure to air, moisture, and/or light,[10,11,7,12–15,9] but whether this degradation arises from physisorbtion[10,11,13,14] or a chemical reaction[6–8,15,9] remains an open question. Although optical absorption[7] and recent X-ray photoelectron spectroscopy[16,15] studies have provided more definitive evidence of a chemical transformation in aged transistor films, the relationship between the observed reaction products and trapped species remains unclear.

Here, we introduce a new spectroscopic method for microscopically probing the electronic states of long-lived trapped charged species in a π-conjugated film,and apply the method to record local trap-clearing action spectra in pentacene for the first time. Pentacene's small size allows us to carry out quantum chemical calculations, which are compared to experiment. Traps in pentacene and a wide-variety of organic semiconductors exhibit a similar 0.6 eV activation energy and, it has been suggested, may therefore share a common trapping mechanism.[13] Our results provide spectroscopic evidence for pentacen-6(13H)-one as the most likely trap species in pentacene. Because polyacenes such as pentacene are promising candidates for field-effect transistors[17–20] and solar cells,[21] this finding should be of general interest to the organic electronics community.

To study charge traps in pentacene, electric force microscopy is combined with variable-wavelength light to follow photochemistry at tens-of-molecule sensitivity and high spatial resolution. Electric force microscopy (EFM) is a well-established tool for non-pertubatively imaging[22] the spatial distribution of long-lived charge-traps and measuring the kinetics of charge-trap formation in devices,[23–25,22] but it gives essentially no molecular-level information about the charge-trap species. Here we demonstrate that combining light with EFM yields spectroscopic data that can be used, along with ab initio calculations of optical spectra, to gain new chemical insights into the mechanisms of charge trapping and charge clearing in organic semiconductors. This study was motivated by recent experiments using EFM to study light-induced trap clearing in polymer transistors[26] and to image photoresponse in polymer blends.[27–29]

Trapping in pentacene has been studied previously using bulk techniques[8,9] as well as by EFM,[23,24,2] but the data has led to inconsistent and contradictory conclusions. For example, EFM studies of pentacene transistors have shown charges to trap either in large grain-like regions,[23] at isolated defect sites,[24] or at intragrain regions.[2] In some samples, traps were cleared by irradiation with light having an above bandgap energy,[8] while in other samples light-induced trap clearing was not observed.[2]

With an eye towards resolving some of these contradictory findings, a polycrystalline pentacene transistor was studied using EFM to measure trap-clearing rates during irradiation as a function of the wavelength of the irradiating light. In parallel, trap density, capacitance, and topography were imaged. Here we present evidence that trapped charge significantly modifies local capacitance and we report a spatially and spectrally resolved action spectrum for trap clearing in polycrystalline pentacene. Measurements were taken in a custom built microscope[23,24] modified to maintain samples in high-purity dry nitrogen. Tip voltage modulation and lock-in detection[30] enabled simultaneous imaging of local electrostatic potential and capacitance.

Trapped charge was generated by applying a gate bias stress, V_g, of –60 V for two minutes with the cantilever retracted to a tip–sample separation of 300 nm and the source and drain electrodes grounded. The topographic data in **Figure 1a**,**d** showed

J. L. Luria, K. A. Schwarz, M. J. Jaquith, Prof. J. A. Marohn
Department of Chemistry and Chemical Biology
Cornell University
Ithaca, New York 14853-1301, USA
E-mail: jam99@cornell.edu
K. A. Schwarz, Prof. R. G. Hennig
Department of Materials Science and Engineering
Cornell University
Ithaca, New York 14853-1501, USA

DOI: 10.1002/adma.201003073

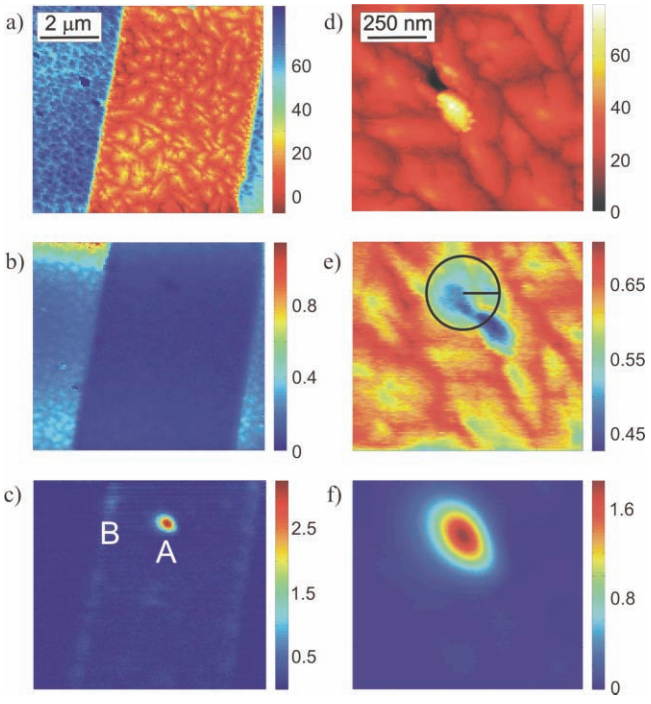

Figure 1. Pentacene transistor channel at low (left, a–c) and high (right, d–f) magnification. a,d) Height in nm; b,e) second derivative with respect to height of tip-sample capacitance (arbitrary units); and c,f) electrostatic potential (V). Points A and B in (c) are two locations exhibiting a high density of trapped charge. The images in (d–f) focus on point A.

regions of low pentacene coverage. Upon bias stress, some of these regions showed suppressed capacitance, indicative of depleted mobile charge; see Figure 1b,e. The same regions also displayed an enhanced electrostatic potential due to trapped charge[26,23,24,22] (Figure 1c,f). Since the sample had been exposed to air, it is plausible that pentacene molecules near the transistor's active layer reacted with air to form an impurity.[6,16,9,15] We suggest that this impurity subsequently reacts in the presence of the holes introduced during bias stress to form a long-lived cationic species. The observed distribution of trapped charge is also consistent with grain boundary or dielectric trapping. Below we use spectroscopic trap clearing data to distinguish between these possibilities.

The suppression of local capacitance by trapped charge in a film of π-conjugated molecules is an effect that has not, to our knowledge, been reported before. The suppressed capacitance highlighted in Figure 1e is a consequence, we suggest, of the Coulombic repulsion of mobile carriers by trapped charge. For simplicity, the trapped charge at position A in Figure 1c,e is modeled as due to a number, N_{trap}, of charges confined to a point and embedded in a material with relative dielectric constant $\varepsilon_r = 3.4$. Calculating the radius of the depleted-capacitance region as the distance, R_{kT}, at which the electrostatic potential from this point charge decays to $\phi(R_{kT}) = kT/q_e = 0.026$ V, we find

$$R_{kT} = \frac{q_e^2 N_{trap}}{4\pi\epsilon_0\epsilon_r kT}. \quad (1)$$

Using Equation 1, it is estimated that $N_{trap} \approx 10$ trapped charges led to the observed $R_{kT} \approx 160$ nm (the circle in Figure 1e). As a check, using the same point-charge model to calculate the potential at a height 60 nm above N_{trap} charges in vacuum gives $\phi = 0.24$ V. This potential is a factor of seven smaller than the 1.6 V apparent in Figure 1f. This order-of-magnitude agreement is reasonable given 1) the lack of an independently validated quantitative theory of the cantilever frequency shift arising from trapped charges[31,32] and 2) the asymmetry apparent in the Figure 1e,f data near the regions of trapped charge, which indicates that the trapped charge is not localized at a single point as the simple model assumes. It is concluded, nevertheless, that Coulombic repulsion is a reasonable model of capacitance depletion and that the position A signal arises from approximately 10 to 100 trapped charges.

To measure the action spectrum of light-induced trap clearing, the cantilever tip was brought over regions of trapped charge in the transistor channel, the sample was illuminated, and the potential drop was observed at each position for ten minutes as a function of the wavelength of light. The potential drop at each wavelength was fit to a first order decay and the decay rate was divided by incident photon energy (eV) to give the constant-incidence action spectrum in units of eV^{-1} s^{-1}. This correction is required because the experiment was performed at constant incident power and not at constant photon flux. The resulting trap-clearing rate per photon may be directly compared to the photocurrent-yield spectrum, which has units of free carriers per photon. The absorption and photocurrent-yield[33] spectra are shown in **Figure 2a** and b, respectively. The detrapping rate is plotted in Figure 2c,d as a function of the irradiated wavelength for points A and B in the sample, respectively.

The clearing of trapped positive charge by light in organic semiconductors is usually attributed to the recombination of trapped holes with excitons,[34] free electrons,[34] or bipolarons.[5] The observation of light-induced trap clearing is usually taken as evidence against trapping due to migration of charge into the dielectric.[35,2] In the excitonic trap-clearing mechanism sketched in **Figure 3a**, light is absorbed to create an exciton (step 1), the excited electron is transferred to an unoccupied state at the trap site (step 2), and the excited hole relaxes and percolates away via electron transfers between adjacent pentacene molecules (step 3). The mid-gap state at the T^+ site in Figure 3a could be a state associated with a grain boundary,[1] a sliding defect,[36] or a valence orbital in pentacene stabilized by dipoles in the nearby dielectric.[3,4] Consistent with the mechanism of Figure 3a, light-enhanced trap clearing was observed at wavelengths where absorption creates either an exciton localized over a single molecule[37] (at 630 nm and 675 nm) or a charge-transfer exciton with intermolecular character[38] (at 575 nm).

In addition to these expected spectral features, the trap-clearing action spectra of Figure 2c,d exhibit a large peak near the wavelength $\lambda = 500$ nm (photon energy $= hc/\lambda = 2.5$ eV). This finding is surprising for two reasons. First, the peak energy is well-above the bandgap of pentacene so that both absorption and photocurrent yield are negligible at this energy and the widely accepted mechanism of Figure 3a can not be applied. Second, even though signal is detected from many charges in different microstructural and electrostatic environments,

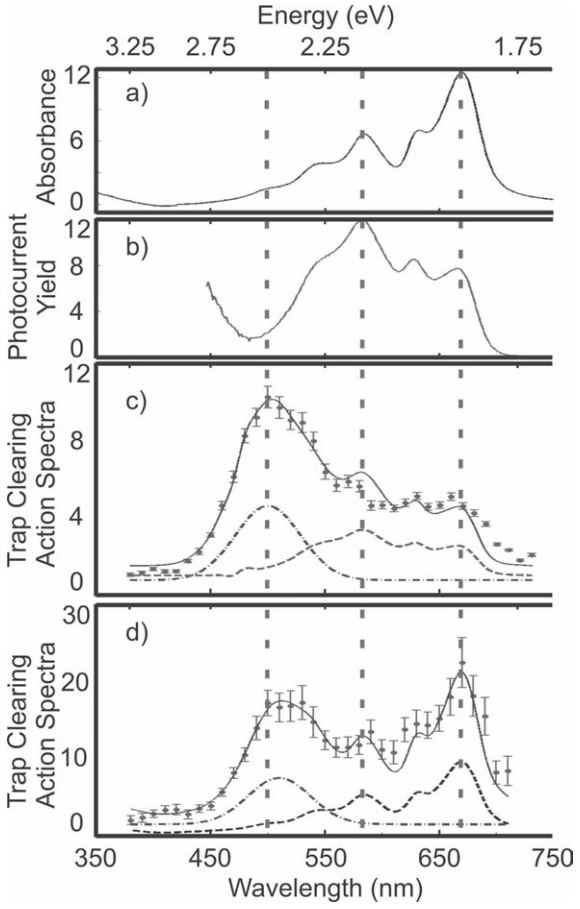

Figure 2. a) Absorbance (scale: arbitrary units) and b) photocurrent yield[33] of bulk pentacene (scale: 10^{-4}). trap-clearing action spectrum acquired at c) location A and d) location B of Figure 1c (circles; scale: 10^{-3} eV^{-1} s^{-1}). The solid line in (c) is a fit to a linear combination of the photocurrent spectrum (dashed line) and a Gaussian (dash-dotted line; center = 2.48 eV, width = 0.14 eV). The solid line in (d) is a fit to the absorption spectrum (dashed line) plus a Gaussian (dash-dotted line; center = 2.43 eV, width = 0.13 eV).

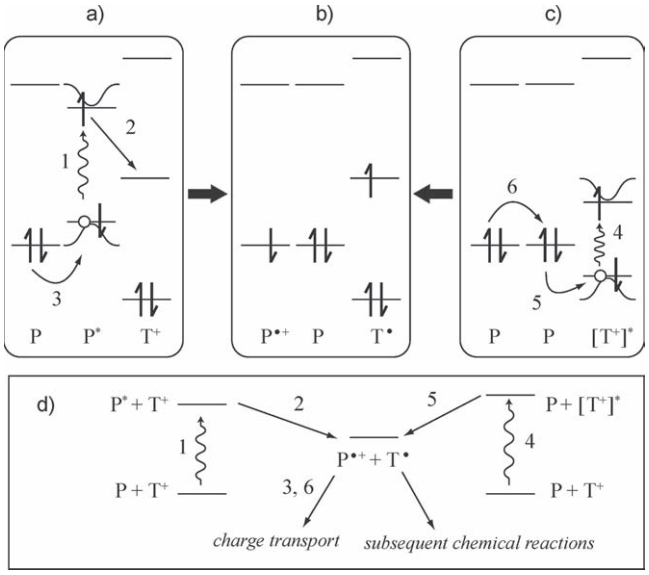

Figure 3. Trap-clearing mechanisms. Here P indicates pentacene, P^* is photoexcited pentacene, and $P^{\bullet+}$ is the pentacene cation radical. The trapped species appears as a neutral radical, $T^{\bullet}$, charged, T^+, or photoexcited and charged, $[T^+]^*$. In (a), a pentacene molecule near a charged trap absorbs light (step 1). Trap-assisted exciton splitting (step 2) populates the trap with an electron and puts a hole onto pentacene, which may be converted to a free hole via charge transfer to a distal pentacene (step 3) to yield the charge-liberated configuration shown in (b). In (c), the cationic trap species is photoexcited directly (step 4) and the trapped hole is released via electron transfer from an adjacent pentacene (step 5). Charge transfer to a distal pentacene (step 6) yields configuration (b). Both trap-clearing mechanisms are summarized in the state diagram in (d).

a comparatively narrow and well-defined trap-clearing action spectrum is observed.

To account for these experimental observations, an alternative trap-clearing mechanism is proposed. In Figure 3c, trap clearing by another kind of photoinitiated electron transfer is shown. In step 4 of the figure, a positively charged chemical impurity is optically excited. The optical excitation does not necessarily have to be the lowest energy excitation. The trap is cleared in step 5 via backfilling through an electron transfer from a nearby pentacene molecule and the resulting hole is transported away (step 6).

A state diagram summarizing the two mechanisms is shown in Figure 3d. This figure highlights that the neutral, open-shell $T^{\bullet}$ species resulting from both trap-clearing mechanisms may undergo further chemical reactions to yield a neutral, closed-shell trap precursor (see Supporting Information). This observation supports conjecture of Lang et al. that atomic motion plays a key role in the quenching of charge traps.[8]

To explain the observed trap-clearing action spectrum by the mechanism of Figure 3c, an impurity or defect in the pentacene solid must be present that exhibits an optical excitation near 500 nm. Time-dependent density functional theory (TDDFT) was used to calculate the optical spectra for two defects proposed as hole traps[6] (shown in **Figure 4**) as well as for pentacene. These two charged defects are the expected products of the reaction of pentacene cation radicals (e.g., holes) with the neutral trap precursors 6,13-dihydropentacene and pentacen-6(13H)-one impurities, respectively.[6] In the calculations a dielectric continuum model was used to describe the surrounding pentacene molecules. While TDDFT is less accurate for certain excitations in gas-phase acene molecules,[39,40] using TDDFT to calculate the energies of a molecule embedded in a dielectric continuum has been shown to accurately describe excitations in the bulk acenes[41] (Supporting Information). More accurate calculations, such as the GW approximation for the Bethe–Salpeter equation (GW-BSE),[42] are computationally very expensive for defect calculations and beyond the scope of this paper.

The solid black lines in Figure 4 show the TDDFT spectra computed using a Gaussian broadening and the TDDFT oscillator strengths for the amplitudes. As seen in Figure 4a, the calculation correctly predicts the peak at 675 nm in the pentacene absorption spectrum. Figure 4b shows that the oxygen defect has a predicted absorption near $\lambda \approx 500$ nm while the hydrogen defect does not. This finding indicates that the oxygen defect and not the hydrogen defect is the source of the unexpected above bandgap peak

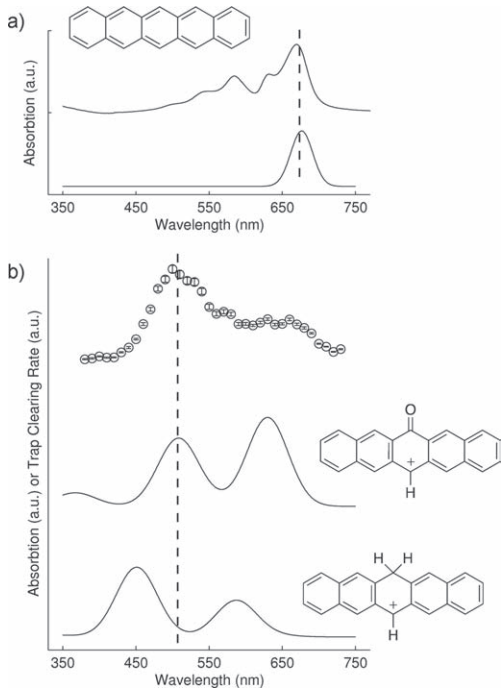

Figure 4. Measured and predicted spectra. a) Pentacene absorption spectrum: measured (upper solid line) and calculated (lower solid line). The calculated spectrum was broadened by 15 nm. b) Measured trap-clearing spectrum (upper solid circles with error bars) and the calculated absorption spectrum for the charged oxygen defect (middle line) and the charged hydrogen defect (lower line). The middle and lower curves were generated by broadening the calculated absorption spectra by 28 nm. The dotted vertical lines are a guide to the eye.

observed in the trap-clearing spectra of Figure 2c,d. The lack of a similarly intense trap-clearing peak at 630 nm can be rationalized in terms of the mechanism of Figure 3c by considering that trap clearing depends on intermolecular electron transfer as well as on absorption (see Supporting Information).

In summary, time- and wavelength-resolved EFM was used to observe local effects of trapped charge on free carriers, to mechanically detect the electronic spectra of tens of molecules, and to uncover new mechanisms of light-induced trap clearing in polycrystalline pentacene. Previously proposed mechanisms of trapping and detrapping involving midgap states at intragrain regions,[1,2] the formation of immobile bipolarons,[5] molecular sliding,[36] the migration of charge into dielectric layers,[2] the stabilization of charges by dipoles in dielectric layers,[3,4] or chemical reactions in the bulk[6–9] cannot simultaneously explain the spatial distribution of traps and the wavelength dependence of trap clearing observed here. A new mechanism of trap clearing via photoexcitation of the trap species followed by electron transfer was suggested; the spectroscopic trap-clearing data implicate pentacen-6(13H)-one as the relevant neutral trap precursor. The experimental technique introduced here opens up exciting possibilities for obtaining electronic spectra of charged trace impurities in films of π-conjugated molecules. Particularly when augmented by ab initio theory, this technique is likely to yield much insight into the chemical identity of defects in organic electronic materials.

Experimental Section

Experimental Sample Preparation Methods: Bottom-contact back-gated transistor substrates were prepared by growing 315 nm of SiO_2 on an n^+ silicon wafer and depositing gold source and drain electrodes by thermal evaporation (5 µm gap). Substrates were sonicated in detergent, dried, cleaned in UV-ozone for five minutes, transferred to high vacuum, and heated to 60 °C; pentacene (Sigma-Aldrich, USA; used as received) was thermally evaporated at a rate of ≈0.1 Å s^{-1} to an average thickness of 15 nm. Completed pentacene field-effect transistors were stored in air and in the dark for a few weeks before being transferred for study to a custom scanned probe microscope housed in a dry-nitrogen box. No current was run through the samples while they were stored in air.

DFT and TDDFT Calculations: Density functional theory (DFT) and time dependent density functional theory (TDDFT) calculations were performed using Gaussian 09[43,44] with the B3LYP[45] functional and the 6-311++G(d,p) basis. The basis set was converged using the frequency of pentacene's first singlet excited state. Changes in this value were less than 4 nm (≈0.01 eV) for the 6-311++G(d,p) compared to the 6-311+G(d) basis. Defect molecule geometries and ground state energies were found by optimizing single-defect molecule geometries with the 6-311++G(d,p) basis and B3LYP. To approximate the chemical environment of the pentacene molecular solid, DFT and TDDFT calculations were performed with solvation in a dielectric medium using the polarizable continuum model (PCM)[46] with a dielectric constant of 4.82, as suggested by previous calculations.[41] Dielectric constants from 3 to 6 were examined and the calculated first singlet excitation frequency in pentacene was found to vary by no more than a few nanometers.

Electric Force Microscopy Methods: Transistor source and drain electrodes were grounded during atomic force microscope, electric force microscope, and trap-clearing spectroscopic measurements. Cantilevers were obtained from SPMTips, USA, (spring constant k = 1 N m^{-1}, resonant frequency f_c = 60 kHz, quality factor Q = 300) and were used for both tapping-mode atomic force microscopy (AFM) and EFM images. Cantilever displacement was detected with a fiber optic interferometer operating at 1310 nm. For EFM experiments, both a direct current (DC) and an alternating current (AC) voltage were applied to the cantilever. The AC voltage had a zero-to-peak amplitude of V_m = 3 V and a frequency of f_m = 200 Hz. EFM images were acquired with a cantilever peak-to-peak oscillation amplitude of 310 nm and a fixed tip–sample separation of 60 nm. The cantilever oscillation was analyzed using a commercial frequency demodulator (RHK, USA; PLLpro 1.0; output bandwidth of 400 Hz), which produced an output proportional to the deviation in the cantilever frequency δf_c. Fourier components of the cantilever frequency deviation were detected at the first and second harmonics of the modulation frequency using lock-in detectors operating at 1 V sensitivity, with time constants of 30 ms (Stanford Research Systems, USA, SR830) and 50 ms (Perkin Elmer, USA; 7265), respectively. The DC voltage was was adjusted via feedback to keep the Fourier component $FT\{\delta f_c\}(f_m)$ equal to zero; the required tip voltage equals the local electrostatic potential displayed in Figure 1c,f. This feedback was accomplished using a commercial analog feedback controller (Stanford Research Systems SIM960, with proportional, integral, and derivative constants of 0.1, 500 Hz, and 0.05 ms, respectively). The second derivative of the tip–sample capacitance, C, with respect to the tip–sample separation, z, displayed in Figure 1b,c was obtained from the measured second harmonic of the cantilever frequency deviation using $\partial^2 C/\partial z^2 = 8k\, FT\{\delta f_c\}(2f_m)/f_c V^2_m$.

To illuminate the sample, an optical fiber of diameter 50 µm and numerical aperture NA = 0.22 was positioned roughly 200 micrometers away from the cantilever tip, inclined at an angle of 30 degrees from horizontal. Visible light with an intensity of 0.015 µW cm^{-2} and a bandwidth of 5 nm was projected down the fiber. The resulting intensity and spectral irradiance at the sample were estimated to be 0.03 mW cm^{-2} and 0.006 mW cm^{-2} nm^{-1}, respectively.

Absorbance and Photocurrent Yield Spectra: The sample used to acquire the absorbance spectrum of Figure 2a was 40 nm of pentacene evaporated on a glass slide. Photocurrent yield measurements[33] (Figure 2b) were conducted on a top-electrode, bottom-gate thin-film

transistor with a 100-nm-thick pentacene layer on 500 nm of thermally grown oxide. Gold electrodes (0.1 mm channel length, 3 mm channel width) were evaporated on pentacene deposited at a rate of 0.4 Å s^{-1} in high vacuum. Photocurrent was generated using a tungsten-halogen lamp, passed through a 0.5 nm resolution monochrometer.

Supporting Information

Supporting Information is available from the Wiley Online Library or from the author. Transistor current-voltage data; additional topographic, capacitance, and electrostatic potential images; representative potential transients; photocurrent and absorption experimental details; reaction mechanisms; and TDDFT calculation details and results are included.

Acknowledgements

We acknowledge Y.-F. Lim and G. G. Malliaras (Cornell University) for the absorbance spectrum and use of a vacuum deposition chamber, M. Breban and E. D. Williams (University of Maryland, College Park) for the photocurrent spectrum,[33] W. R. Dichtel (Cornell University) for discussions of polyacene chemistry, and G. K.-L. Chan (Cornell University) for advice on electronic structure calculations. We acknowledge the NSF (DMR-0706508, ECS-0335765, EAR-0703226, and a Graduate Research Fellowship) and the DOE (DE-FG05-08OR23339) for support. Computational resources were provided by NCSA, NERSC, and CCNI.

Received: August 24, 2010
Revised: September 29, 2010
Published online: December 6, 2010

[1] S. Verlaak, V. Arkhipov, P. Heremans, *Appl. Phys. Lett.* **2003**, *82*, 745.
[2] M. Tello, M. Chiesa, C. M. Duffy, H. Sirringhaus, *Adv. Funct. Mater.* **2008**, *18*, 3907.
[3] J. Veres, S. Ogier, G. Lloyd, D. De Leeuw, *Chem. Mater.* **2004**, *16*, 4543.
[4] S. J. Konezny, M. N. Bussac, L. Zuppiroli, *Phys. Rev. B* **2010**, *81*, 045313.
[5] R. Street, A. Salleo, M. Chabinyc, *Phys. Rev. B* **2003**, *68*, 85316.
[6] J. E. Northrup, M. L. Chabinyc, *Phys. Rev. B* **2003**, *68*, 041202.
[7] A. Maliakal, K. Raghavachari, H. Katz, E. Chandross, T. Siegrist, *Chem. Mater.* **2004**, *16*, 4980.
[8] D. V. Lang, X. Chi, T. Siegrist, A. M. Sergent, A. P. Ramirez, *Phys. Rev. Lett.* **2004**, *93*, 076601.
[9] D. Knipp, J. E. Northrup, *Adv. Mater.* **2009**, *21*, 2511.
[10] Z. T. Zhu, J. T. Mason, R. Dieckmann, G. G. Malliaras, *Appl. Phys. Lett.* **2002**, *81*, 4643.
[11] Y. Qiu, Y. C. Hu, G. F. Dong, L. D. Wang, J. F. Xie, Y. N. Ma, *Appl. Phys. Lett.* **2003**, *83*, 1644.
[12] C. Pannemann, T. Diekmann, U. Hilleringmann, *J. Mater. Res.* **2004**, *19*, 1999.
[13] S. G. J. Mathijssen, M. Cölle, H. Gomes, E. C. P. Smits, B. de Boer, I. McCulloch, P. A. Bobbert, D. M. de Leeuw, *Adv. Mater.* **2007**, *19*, 2785.
[14] G. Gu, M. G. Kane, *Appl. Phys. Lett.* **2008**, *92*, 053305.
[15] H. Yang, L. Yang, M.-M. Ling, S. Lastella, D. D. Gandhi, G. Ramanath, Z. Bao, C. V. Ryu, *J. Phys. Chem. C* **2008**, *112*, 16161.
[16] A. Vollmer, O. Jurchescu, I. Arfaoui, I. Salzmann, T. Palstra, P. Rudolf, J. Niemax, J. Pflaum, J. Rabe, N. Koch, *Eur. Phys. J. E* **2005**, *17*, 339.
[17] Y. Y. Lin, D. J. Gundlach, S. F. Nelson, T. N. Jackson, *IEEE Trans. Electron Devices* **1997**, *44*, 1325.
[18] J. E. Anthony, *Chem. Rev.* **2006**, *106*, 5028.
[19] R. A. Street, *Adv. Mater.* **2009**, *21*, 2007.
[20] M. J. Jaquith, J. E. Anthony, J. A. Marohn, *J. Mater. Chem.* **2009**, *19*, 6116.
[21] S. Yoo, B. Domercq, B. Kippelen, *Appl. Phys. Lett.* **2004**, *85*, 5427.
[22] T. N. Ng, J. A. Marohn, M. L. Chabinyc, *J. Appl. Phys.* **2006**, *100*, 084505.
[23] E. M. Muller, J. A. Marohn, *Adv. Mater.* **2005**, *17*, 1410.
[24] M. Jaquith, E. M. Muller, J. A. Marohn, *J. Phys. Chem. B* **2007**, *111*, 7711.
[25] T. N. Ng, W. Silveira, J. Marohn, *Proc. SPIE* **2006**, *6336*, 63360A.
[26] L. Bürgi, T. Richards, M. Chiesa, R. H. Friend, H. Sirringhaus, *Synth. Met.* **2004**, *146*, 297.
[27] H. Hoppe, T. Glatzel, M. Niggemann, A. Hinsch, M. C. Lux-Steiner, N. S. Sariciftci, *Nano Lett.* **2005**, *5*, 269.
[28] M. Chiesa, L. Bürgi, J. S. Kim, R. Shikler, R. H. Friend, H. Sirringhaus, *Nano Lett.* **2005**, *5*, 559.
[29] D. C. Coffey, D. S. Ginger, *Nat. Mater.* **2006**, *5*, 735.
[30] A. Kikukawa, S. Hosaka, R. Imura, *Appl. Phys. Lett.* **1995**, *66*, 3510.
[31] W. R. Silveira, E. M. Muller, T.-N. Ng, D. H. Dunlap, J. A. Marohn in *Scanning Probe Microscopy: Electrical and Electromechanical Phenomena at the Nanoscale (Volume II)*, (Eds: S. V. Kalinin, A. Gruverman), Springer Verlag, New York **2007**; pp. 788.
[32] A. Liscio, V. Palermo, P. Samori, *Acc. Chem. Res.* **2010**, *43*, 541.
[33] M. Breban, D. B. Romero, S. Mezhenny, V. W. Ballarotto, E. D. Williams, *Appl. Phys. Lett.* **2005**, *87*, 203503.
[34] A. Salleo, R. A. Street, *J. Appl. Phys.* **2003**, *94*, 471.
[35] A. Salleo, F. Endicott, R. A. Street, *Appl. Phys. Lett.* **2005**, *86*, 263505.
[36] J. H. Kang, D. da Silva, J. L. Bredas, X. Y. Zhu, *Appl. Phys. Lett.* **2005**, *86*, 152115.
[37] C. Jundt, G. Klein, B. Sipp, J. Lemoigne, M. Joucla, A. A. Villaeys, *Chem. Phys. Lett.* **1995**, *241*, 84.
[38] L. Sebastian, G. Weiser, H. Bässler, *Chem. Phys.* **1981**, *61*, 125.
[39] S. Grimme, M. Parac, *Chem. Phys. Chem.* **2003**, *4*, 292.
[40] E. S. Kadantsev, M. J. Stott, A. Rubio, *J. Chem. Phys.* **2006**, *124*, 134901.
[41] P. K. Nayak, N. Periasamy, *Org. Electron.* **2009**, *10*, 1396.
[42] M. L. Tiago, J. E. Northrup, S. G. Louie, *Phys. Rev. B* **2003**, *67*, 115212.
[43] *Gaussian 09, Revision A.1*; M. J. Frisch, G. W. Trucks, H. B. Schlegel, G. E. Scuseria, M. A. Robb, J. R. Cheeseman, G. Scalmani, V. Barone, B. Mennucci, G. A. Petersson, H. Nakatsuji, M. Caricato, X. Li, H. P. Hratchian, A. F. Izmaylov, J. Bloino, G. Zheng, J. L. Sonnenberg, M. Hada, M. Ehara, K. Toyota, R. Fukuda, J. Hasegawa, M. Ishida, T. Nakajima, Y. Honda, O. Kitao, H. Nakai, T. Vreven, J. A. Montgomery, Jr., J. E. Peralta, F. Ogliaro, M. Bearpark, J. J. Heyd, E. Brothers, K. N. Kudin, V. N. Staroverov, R. Kobayashi, J. Normand, K. Raghavachari, A. Rendell, J. C. Burant, S. S. Iyengar, J. Tomasi, M. Cossi, N. Rega, J. M. Millam, M. Klene, J. E. Knox, J. B. Cross, V. Bakken, C. Adamo, J. Jaramillo, R. Gomperts, R. E. Stratmann, O. Yazyev, A. J. Austin, R. Cammi, C. Pomelli, J. W. Ochterski, R. L. Martin, K. Morokuma, V. G. Zakrzewski, G. A. Voth, P. Salvador, J. J. Dannenberg, S. Dapprich, A. D. Daniels, Ö. Farkas, J. B. Foresman, J. V. Ortiz, J. Cioslowski, D. J. Fox, Gaussian Inc., Wallingford, CT, **2009**.
[44] R. Bauernschmitt, R. Ahlrichs, *Chem. Phys. Lett.* **1996**, *256*, 454.
[45] A. D. Becke, *J. Chem. Phys.* **1993**, *98*, 5648.
[46] S. Miertus, E. Scrocco, J. Tomasi, *Chem. Phys.* **1981**, *55*, 117.